Electronic Supplementary Material (ESI) for Energy Advances.

Supporting Information

Low-intensity low-temperature analysis of perovskite solar cells for deep space applications

Tyler Colenbrander,[a] Jun Peng,[b] Yiliang Wu,[b] Michael Kelzenberg,[c] Jing-Shun Huang,[d] Clara MacFarland,[a] Dennis Thorbourn,[a] Robert Kowalczyk,[a] Wousik Kim,[a] John Brophy,[a] Anh Dinh Bui,[b] Dang-Thuan Nguyen,[b] Hieu T. Nguyen,[b] Harry A. Atwater,[c] Thomas White,[b] and Jonathan Grandidier*[a]

[a] Jet Propulsion Laboratory, California Institute of Technology, Pasadena, CA 91109, USA
E-mail: jgrandid@gmail.com
[b] School of Engineering, The Australian National University, Canberra, Australian Capital Territory 2601, Australia
[c] Thomas J. Watson Laboratories of Applied Physics, California Institute of Technology, Pasadena, CA 91125, USA
[d] Caelux Corporation, 404 N Halstead Street, Pasadena, CA 91107

Additional Experimental Information

Low-temperature Photoluminescence Measurement Procedure:

PL measurements were performed using a Horiba LabRAM HR Evolution system equipped with confocal optics and a silicon charge-couple-device (CCD) detector. The laser excitation wavelength was 532 nm and the laser light was focused onto the sample surface using a 10x objective (numerical aperture = 0.25) yielding a spot diameter of ≈2.5mm. The on-sample power was kept constant at ≈3 microwatt. The temperature was controlled using a liquid nitrogen Linkam cooling stage (Linkam Scientific Instruments, UK) with a cooling rate of 60 K/minute. After the sample stage reached the set temperature, the sample was held at that temperature for 5 minutes in order to get a uniform thermal distribution before doing the measurements.

Additional Experimental Data

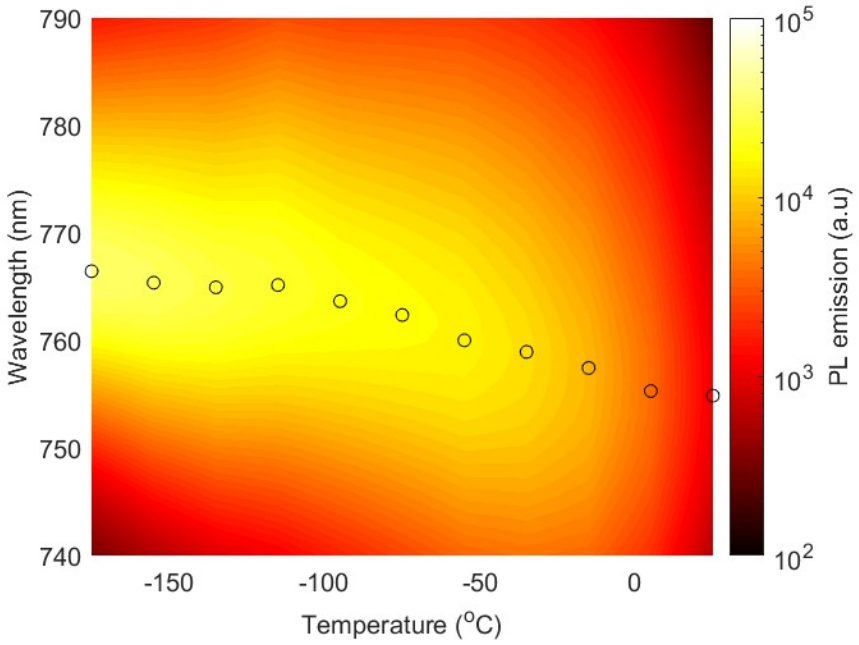

Figure S1. Steady-state photoluminescence emission spectra of perovskite films identical to those used in the ANU cells deposited on glass, measured at temperatures from -175℃ to 25℃. The black circles indicate the peak emission wavelength at each temperature. The increase in PL emission intensity with decreasing temperature is an indication of reduced non-radiative (trap-assisted) carrier recombination.

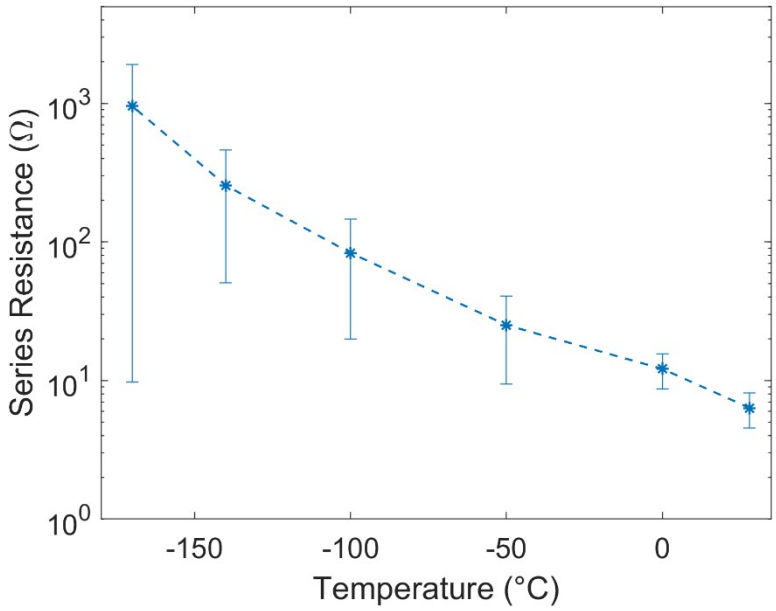

Figure S2. Approximated cell series resistance for n = 7 ANU cell measurements before radiation. The error bars denote the standard deviation in the set of samples. The series resistance is approximated from the J-V curves by estimating the slope of the curve at the open-circuit voltage point. As temperature decreases, the overall series resistance increases, consistent with the decrease in cell efficiency observed in Figure S1. A similar analysis was performed at lower light intensities, but due to the low magnitude of the measured current, the series resistance cannot be accurately approximated by the slope of the J-V curve at the open-circuit voltage point.

Analysis of Outlier Data

The data presented in **Figure 4** of the manuscript is taken from n = 3 perovskite solar cell (PSC) measurements from three different cells labeled ANU9, ANU10, and ANU12. Additional measurements on 4 cells labeled ANU5, ANU7, ANU13, and ANU14 were taken but the resulting data set has outlier data that we suspect comes from current leakage occurring in the sample stage. As expected, the shunting caused by current leakage appears to have a larger effect at the lower light intensities, so the 19.2 AU data is most affected. While all 7 PSCs yielded similar 1.0 AU and 5.5 AU measurements, we observed that 4 cells had unusual J-V curve measurements at 19.2 AU and corresponding much lower efficiencies, indicative of shunting. Thus, we removed these 4 cells from the statistical analysis presented in the manuscript in favor of the three cells. For completeness, the entire n = 7 dataset can be seen in **Figure S1**. The same trends shown in Figure 4 of the manuscript are present, but the 19.2 AU data is clearly different and has much larger standard deviations.

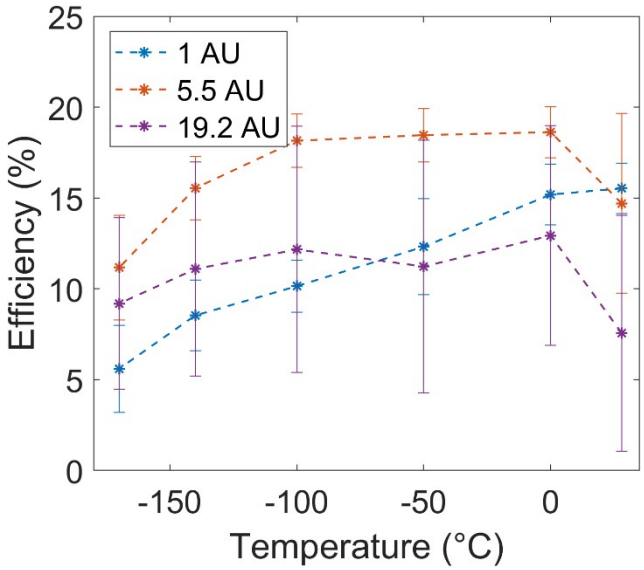

Figure S3. Plots of average efficiency with respect to temperature at various light intensities for n = 7 ANU cell measurements before radiation. The error bars denote the standard deviation in the set of samples.

Cell Parameters with Respect to Radiation Fluence

Taking one ANU PSC at each radiation fluence, we plot cell parameters with respect to radiation fluence, both in the standard 1.0 AU, 28℃ conditions and in the extreme LILT 19.2 AU, -170℃ conditions. The cells corresponding to radiation fluences of 0 (control), 4.32×10^{13} p+/cm^2, 8.64×10^{13} p+/cm^2, 1.30×10^{14} p+/cm^2, and 1.73×10^{14} p+/cm^2 are labeled ANU10, ANU9, ANU13, ANU5, and ANU12, respectively. As noted in the analysis of outlier data, cells ANU9, ANU10, and ANU12 appear to show current shunting through the sample stage at the lowest light intensity of 19.2 AU, which underestimates the cell efficiency. Thus, we cannot claim that efficiency numbers are completely accurate, but the overall trends with respect to radiation fluence remain clear. As expected, efficiency, short-circuit current, and fill factor tend to decrease as fluence increases. This trend in short-circuit current could partially be an effect of the glass darkening or decreased reflection from the back contact, but further studies would be required to provide more insight. The open-circuit voltage remains relatively constant with respect to fluence. When comparing standard (1.0 AU, 28℃) conditions with extreme LILT (19.2 AU, -170℃) conditions, the trends appear similar, but inconsistent data and efficiency degredation is notably more in the extreme LILT conditions, partly due to the shunting concerns presented above. However, the control cell ANU10 has no observed shunting. Notably, the control cell experiences little degredation in the standard conditions (0.91 remaining factor) but much more severe degredation in the extreme LILT conditions (0.60 remaining factor). This suggests that device degredation is not constant with respect to the test conditions, and thus different cell architectures and radiation protection may be optimal depending on mission conditions.

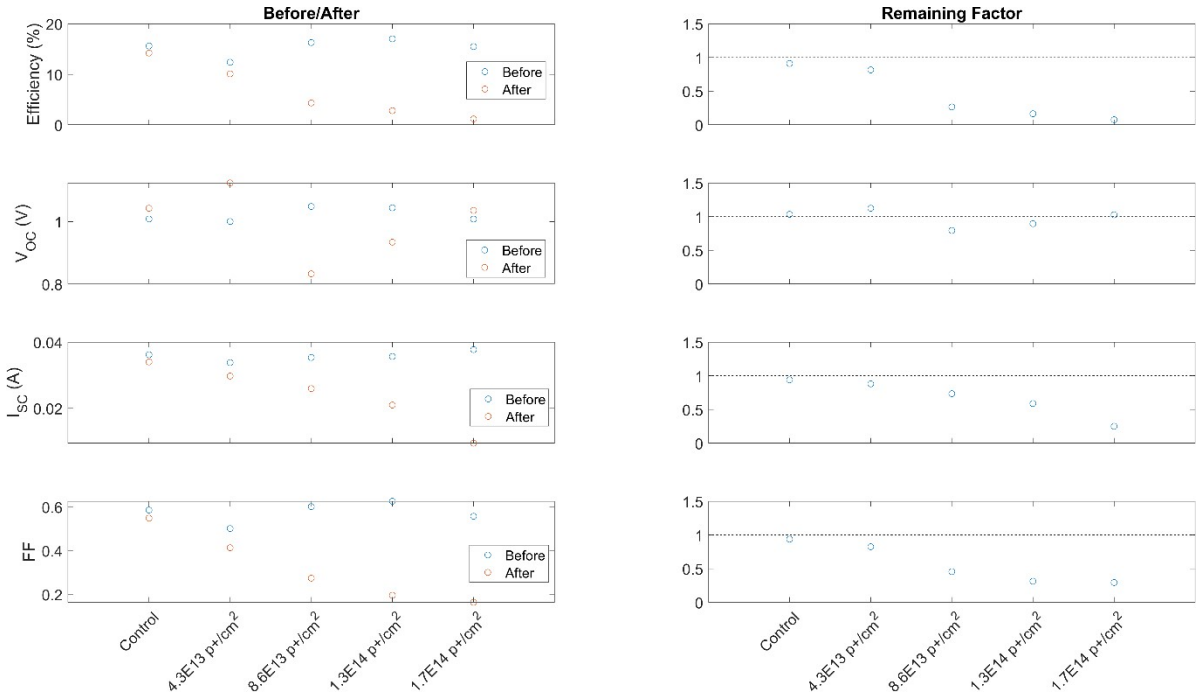

Figure S4. Efficiency (%), open-circuit voltage (V), short-circuit current (A), and fill factor with respect to radiation fluence, measured in 1.0 AU, 28℃ conditions. (left) Before radiation and after radiation comparison. (right) Remaining factor.

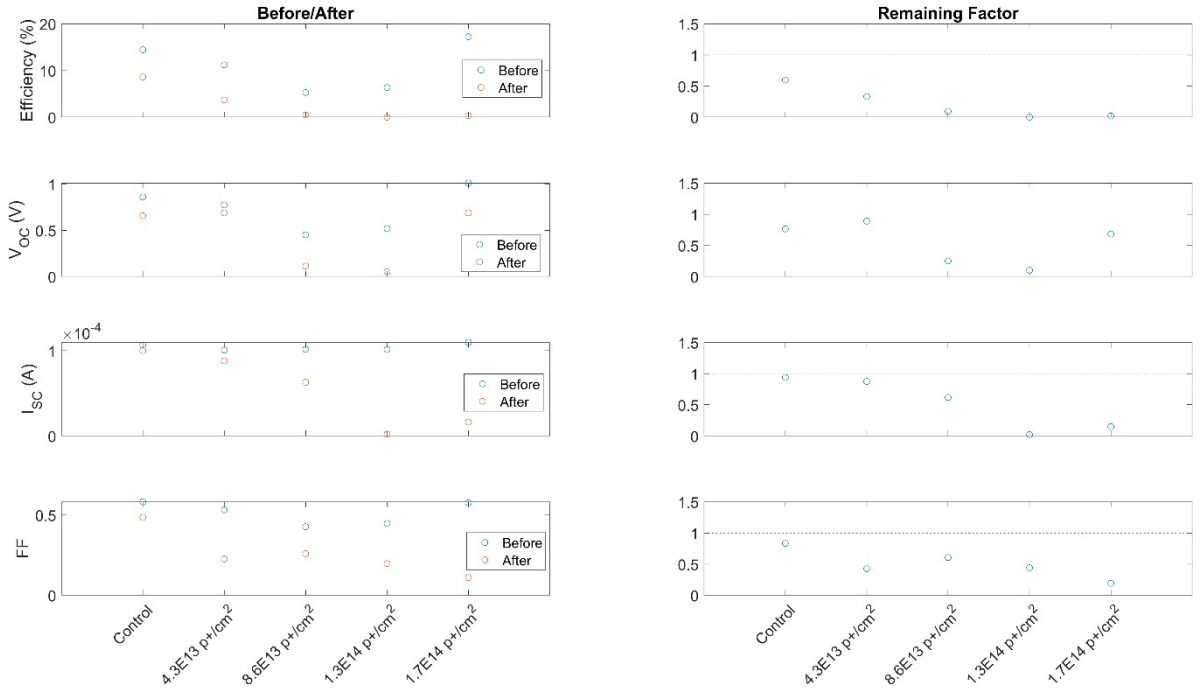

Figure S5. Efficiency (%), open-circuit voltage (V), short-circuit current (A), and fill factor with respect to radiation fluence, measured in 19.2 AU, -170℃ conditions. (left) Before radiation and after radiation comparison. (right) Remaining factor.

Testing reversibility of temperature- induced and light-induced trends

To test the reversibility of temperature-induced and light-induced trends and determine if device degredation played a role in performance change, we performed 28℃ room temperature measurements both before and after subjecting the PSCs to LILT conditions. The resulting measurements (shown here for ANU9) indicate no clear degredation, suggesting that the trends are indeed reversible.

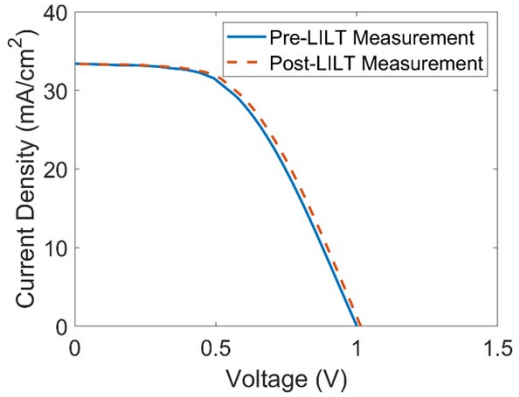

Figure S6. J-V curve for ANU9 cell at 1.0 AU before and after being subjected to low-intensity low-temperature conditions.

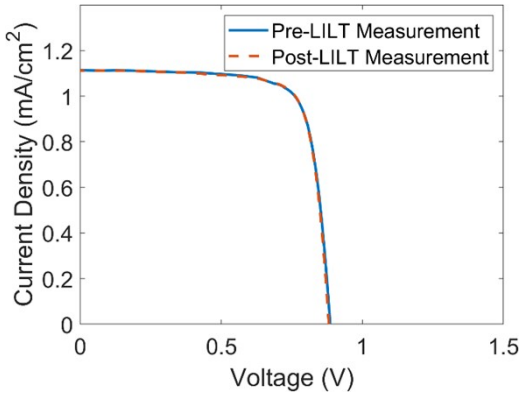

Figure S7. J-V curve for ANU9 cell at 5.5 AU before and after being subjected to low-intensity low-temperature conditions.

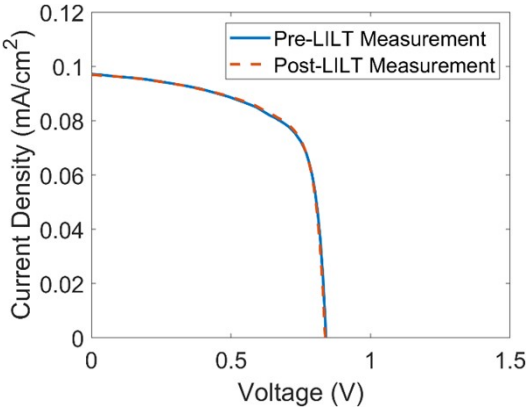

Figure S8. J-V curve for ANU9 cell at 19.2 AU before and after being subjected to low-intensity low-temperature conditions.